CrossMark

ROYAL
AERONAUTICAL
SOCIETY

REGULAR PAPER

Cooperative guidance for active defence based on line-of-sight constraint under a low-speed ratio

S. Liu[1] , Y. Wang[2], Y. Li[2], B. Yan[3,*] and T. Zhang[1]

[1]Unmanned System Research Institute, Northwestern Polytechnical University, Xi'an, China, [2]Shanghai Electro-Mechanical Engineering Institute, Shanghai, China and [3]School of Astronautics, Northwestern Polytechnical University, Xi'an, China
*Corresponding author. Email: yanbinbin@nwpu.edu.cn

Abstract

In this study, an active defence cooperative guidance (ADCG) law that enables cheap and low-speed airborne defence missiles with low manoeuverability to accurately intercept fast and expensive attack missiles with high manoeuverability was designed to enhance the capability of aircraft for active defence. This guidance law relies on the line-of-sight (LOS) guidance method, and it realises active defence by adjusting the geometric LOS relationship involving an attack missile, a defence missile and an aircraft. We use a nonlinear integral sliding surface and an improved second-order sliding mode reaching law to design the guidance law. This can not only reduce the chattering phenomenon in the guidance command, but it can also ensure that the system can reach the sliding surface from any initial position in a finite time. Simulations were carried out to verify the proposed law using four cases: different manoeuvering modes of the aircraft, different speed ratios of the attack and defence missiles, different reaching laws applied to the ADCG law and a robustness analysis. The results show that the proposed guidance law can enable a defence missile to intercept an attack missile by simultaneously using information about the relative motions of the attack missile and the aircraft. It is also highly robust in the presence of errors and noise.

Nomenclature

OXY	inertial coordinate system
R	relative range
λ	line-of-sight angle
γ	path angle
V	speed
a	normal acceleration
A	attack missile
D	defence missile
T	aircraft

1.0 Introduction

In modern air-combat scenarios, it is critical to protect aircraft from attacks. For example, an aircraft may be attacked by hostile missiles during aerial reconnaissance or while carrying combat materials and personnel injured on the battlefield [1]. Aircraft have major disadvantages against attack missiles in terms of flight speed and manoeuverability [2, 3]. In most cases, an aircraft can use passive defence measures to avoid threats, such as by dropping chaff missiles, but this may not always be effective, even if the aircraft has sufficient flight speed and manoeuverability, due to the constraints of its load or

constraints related to the flight mission [4, 5]. Guidance is required to produce the commands to guide a flight vehicle to move a specified trajectory, and, if required, optimises a specific performance [6, 7]. Thus, one alternative is for the aircraft to launch missiles to actively defend itself. In these cases, a guidance law is required that can comprehensively consider the trajectories of both the aircraft and the attack missile to ensure the safety of the former.

Due to its general effectiveness, active defence has been widely studied in the context of defending aircraft. On the premise that the guidance law of an attack missile is a linear law that is known, Shima [8] derived a cooperative guidance law between the defence missile and the aircraft by linearising the equation of their relative motions. Shaferman et al. [9] proposed a multimode adaptive defence missile guidance law by estimating its parameters using a set of filters. However, this method requires selecting an appropriate combination of the guidance law and the relevant parameters of the defence missile from a known and finite set. The size of this set depends on the number of filters, and this limits the application of this guidance law in engineering practice. Prokopov et al. [10] designed three optimal schemes for guiding active defence according to the cooperative modes of the defence missile and the aircraft. These schemes reduce the high-order equation of motion to a first-order dynamic equation with a zero-effort miss formulation, which simplifies the derivation of the guidance law. However, these studies have all been based on optimal control theory, the design of which requires estimating the remaining flying time t_{go}, and the accuracy of this estimation directly affects the accuracy of the attack.

To protect aircraft, defence missiles need to intercept attack missiles; to attack aircraft, attack missiles need to evade this interception. This is essentially a differential game problem. Some studies have thus used differential game theory to solve the problem of active aircraft defence. For example, using the theory of linear quadratic differential games, Perelman et al. [11] examined the game problem involving an attack missile, a defence missile and an aircraft. The original equation of state was reduced by using the terminal projection method, and the closed-loop analytical expression of each guidance strategy was given. On this basis, Saurav et al. [12] designed a linear quadratic differential game-based guidance law with an angle constraint to improve the interception-related performance of the defence missile. Given that the extent of control of the linear quadratic differential game-based guidance law may exceed the set boundary, Rubinsky et al. [13] designed a bounded differential game-based guidance law from the perspective of the attack missile. Based on differential game theory, the work described in Refs. [14] and [15] developed optimal guidance schemes for the attack missile, the defence missile and the aircraft, and the feasible area of interception of the defence missile was analysed according to the aircraft's manoeuvering modes. However, these methods are all fully or partially based on the assumption of linearisation, and they thus have certain limitations. As with optimal guidance schemes, differential game-based guidance laws require estimation of t_{go}, and the accuracy of this estimation again directly influences that of the attack. In addition, as a result of the comprehensive performance index used in its design, the miss distance of the linear quadratic differential game-based guidance law may not be able to reach the appropriate minimum. Weight-related parameters in the performance index are also difficult to determine.

If the attack missile, defence missile and aircraft are abstracted as points in space, the lines connecting them will form a triangle. One feasible guidance strategy is for the defence missile to control itself to be in the line of sight (LOS) of the aircraft, the defence missile and the attack missile so that this triangle is reduced to a straight line. Then, as the attack missile approaches the aircraft, it will be intercepted by the defence missile. Shima et al. [16] proposed a guidance law based on the LOS constraint that included an expression for the acceleration of the attack missile. However, in practice, it is difficult for the defence missile to determine the acceleration of the attack missile. Yamasaki et al. [17] claimed that the guidance command of the defence missile is proportional to two parameters. The first is the difference between the LOS angle formed between the defence missile and the attack missile, and the second is the speed of the defence missile relative to that of the attack missile. For an active defence scenario in which an aircraft launches a defending missile as a counter weapon against an incoming attacking missile, Ratnoo et al. [18] proposed an LOS guidance strategy for the defending missile. Their results demonstrated that the attacker pays the maximum penalty for an evasive manoeuver from the defender if the defender adopts LOS guidance.

Sliding mode control (SMC) has been widely used for designing guidance laws because of its good adaptability and robustness against parametric uncertainty and external disturbances [19]–[21]. Liu et al. [22] designed an impact time control guidance law based on equivalent sliding mode control method with a field-of-view constraint for anti-ship missiles, and this scheme requires no assumption of small angle approximation. By using the three-dimensional kinematic equation set constructed in a rotating coordinate system, Shin et al. [23] designed a finite-time SMC-based guidance law to nullify the LOS angular rate at the interception time. For the terminal guidance problem of missiles intercepting manoeuvering targets in the three-dimensional space, Song et al. [24] studied the design of guidance laws for non-decoupling three-dimensional engagement geometry based on the SMC theory. Sinha et al. [25] made use of the advantages of the super-twisting algorithm to propose a leader–follower cooperative guidance law for intercepting non-manoeuvering targets. This can obtain the time of expected attack in the case of a large lead angle.

Importantly, the above research on active aircraft defence was conducted under the assumption that the flight speed and manoeuverability of the defence missile are superior to those of the attack missile, which imposes stringent requirements on the actuator and the production cost of the defence missile. In this study, we examined the problem of active aircraft defence with the following considerations: (1) we sought to improve the probability of aircraft survival by accurately intercepting a fast, highly manoeuverable, and expensive attack missile using a slow, weakly manoeuverable, and cheap defence missile; (2) we used active defence scenarios to design a cooperative guidance law based on a SMC method that converges quickly and is highly robust.

Based on this research background, we designed an active defence cooperative guidance (ADCG) law based on the LOS constraint with a low speed ratio. This uses a nonlinear integral sliding surface and an improved reaching law to ensure that the directions of the LOS of the attack missile, the defence missile, and the aircraft are in a straight line at the time of interception to protect the aircraft. The main contributions of this paper can be summarised as follows.

1. An active defence cooperative guidance law based on the LOS constraint is proposed; in contrast to previous research [16]–[18], this considers an active defence scenario in which the flight speeds of the defence missile and the aircraft are lower than that of the attack missile. The defence missile simultaneously uses information about the movement of the attack missile, the defence missile and the aircraft to protect the aircraft during flight.

2. In contrast to previous research [22] and [26], the ADCG law is formulated based on a nonlinear integral sliding surface by using an improved reaching law. This improves the closed-loop error dynamic of the guidance system such that the guidance command features no chattering, and it enables the system to reach the sliding surface from any initial position in a finite time.

The remainder of this paper is organised as follows: Section 2 addresses the problem of active defence in the longitudinal plane in the terminal guidance stage; the design of the guidance law is outlined in Section 3, and a stability analysis is given in Section 4; comparative simulation studies are presented in Section 5, and conclusions are drawn in Section 6.

2.0 Problem description

To accurately analyse a confrontation involving an attack missile (A), a defence missile (D) and an aircraft (T) and solve for the guidance law of the defence missile, the relative motions of all three need be modeled and analysed. This relationship is shown in the longitudinal plane in the terminal guidance stage in Fig. 1.

In Fig. 1, *OXY* represents the inertial coordinate system. The relative ranges of movement of the attack missile, the defence missile, and the aircraft are denoted by R_{AT}, R_{AD}, and R_{DT}, respectively, and their LOS angles are denoted by λ_{AT}, λ_{AD}, and λ_{DT}. $V_i(i=T, D, A)$ represents their speeds, $a_i(i=T, D, A)$ represents their normal accelerations, which are perpendicular to the directions of their respective speeds, and $\gamma_i(i=T, D, A)$ represents their path angles.
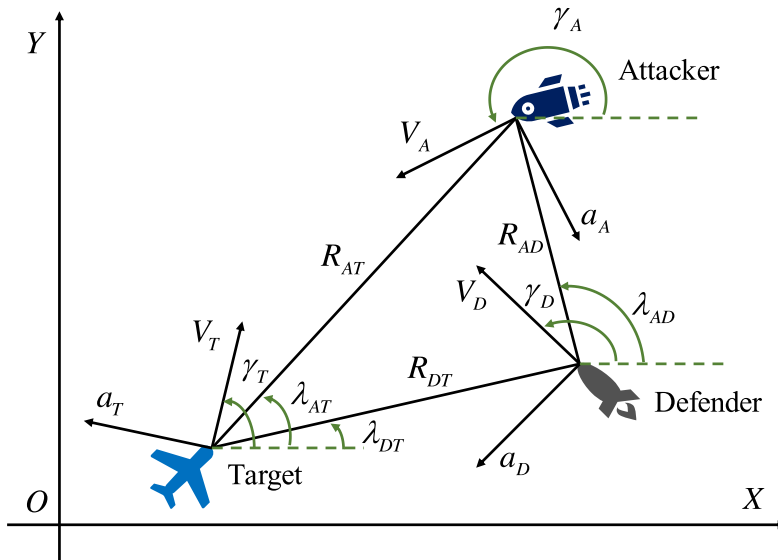
Figure 1. *Engagement geometry.*

As shown in Fig. 1, the relative motions of the attack missile, defence missile, and aircraft under the LOS system can be expressed as:

$$\dot{R}_{AT} = V_A \cos(\gamma_A - \lambda_{AT}) - V_T \cos(\gamma_T - \lambda_{AT}) \tag{1}$$

$$\dot{R}_{AD} = V_A \cos(\gamma_A - \lambda_{AD}) - V_D \cos(\gamma_D - \lambda_{AD}) \tag{2}$$

$$\dot{R}_{DT} = V_D \cos(\gamma_D - \lambda_{DT}) - V_T \cos(\gamma_T - \lambda_{DT}) \tag{3}$$

$$R_{AT}\dot{\lambda}_{AT} = V_A \sin(\gamma_A - \lambda_{AT}) - V_T \sin(\gamma_T - \lambda_{AT}) \tag{4}$$

$$R_{AD}\dot{\lambda}_{AD} = V_A \sin(\gamma_A - \lambda_{AD}) - V_D \sin(\gamma_D - \lambda_{AD}) \tag{5}$$

$$R_{DT}\dot{\lambda}_{DT} = V_D \sin(\gamma_D - \lambda_{DT}) - V_T \sin(\gamma_T - \lambda_{DT}) \tag{6}$$

where their speeds satisfy $V_T < V_D < V_A$. As noted, the aircraft and the defence missile are slower than the attack missile.

The kinematics of the attack missile, defence missile, and aircraft in the inertial coordinate system can be expressed as:

$$\dot{X}_i = V_i \cos\gamma_i (i = A, D, T) \tag{7}$$

$$\dot{Y}_i = V_i \sin\gamma_i (i = A, D, T) \tag{8}$$

Assuming that they all have an ideal autopilot and manoeuvering dynamics with upper bounds of manoeuverability,

$$\dot{\gamma}_i = \frac{a_i}{V_i}(i = A, D, T) \tag{9}$$
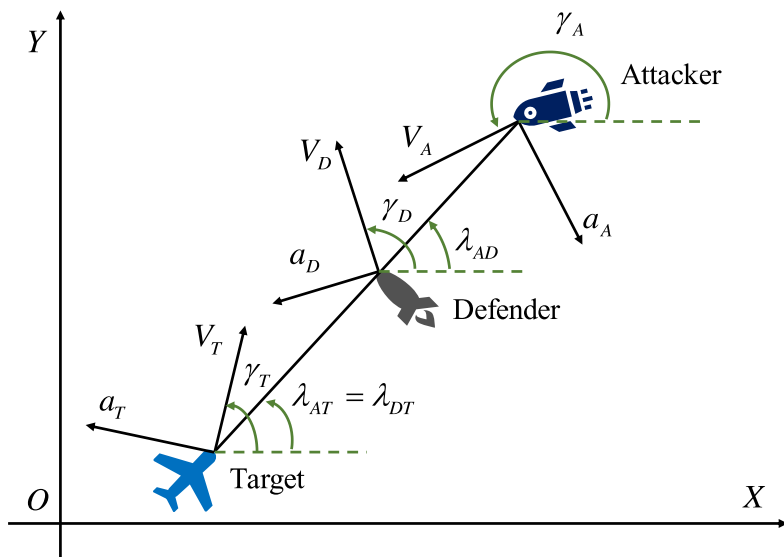
$$|a_i| \leq a_i^{\max} \tag{10}$$

Figure 2. *Ideal engagement geometry.*

where $a_i^{\max}(i = A, D, T)$ represents the upper bound of their respective manoeuverability, satisfying $a_T^{\max} < a_D^{\max} < a_A^{\max}$. In other words, in comparison with the attack missile, the aircraft and the defence missile have inferior manoeuverability.

We also assume that the speeds of the attack missile, defence missile, and aircraft remain unchanged, which means that $a_i(i = A, D, T)$ changes only their directions. Thus, the derivatives of Equations (4)-(5) can be obtained as:

$$\ddot{\lambda}_{AD} = -\frac{2\dot{R}_{AD}\dot{\lambda}_{AD}}{R_{AD}} - \frac{a_D \cos(\gamma_D - \lambda_{AD})}{R_{AD}} + \frac{a_A \cos(\gamma_A - \lambda_{AD})}{R_{AD}} \tag{11}$$

$$\ddot{\lambda}_{AT} = -\frac{2\dot{R}_{AT}\dot{\lambda}_{AT}}{R_{AT}} + \frac{a_A \cos(\gamma_A - \lambda_{AT})}{R_{AT}} - \frac{a_T \cos(\gamma_T - \lambda_{AT})}{R_{AT}} \tag{12}$$

where $a_A \cos(\gamma_A - \lambda_{AD})$ represents the component of acceleration of the attack missile normal to the LOS of R_{AD}, and $a_T \cos(\gamma_T - \lambda_{AT})$ represents that of the aircraft normal to the LOS of R_{AT}.

Based on Equation (10), we assume that there are upper bounds $\Delta_{AD}^{\max}$ and $\Delta_{AT}^{\max}$ for $\Delta_{AD} = a_A \cos(\gamma_A - \lambda_{AD})/R_{AD}$ and $\Delta_{AT} = a_T \cos(\gamma_T - \lambda_{AT})/R_{AT}$, respectively, and we regard Δ_{AD} and Δ_{AT} as their respective external disturbances or uncertainties. Then,

$$|\Delta_{AD}| \leq \Delta_{AD}^{\max} \tag{13}$$

$$|\Delta_{AT}| \leq \Delta_{AT}^{\max} \tag{14}$$

To protect the aircraft from the attack missile, the defence missile needs to accurately intercept it. Regardless of how it is guided, once the defence missile has been launched, it must fly toward the attack missile. In the face of an attack missile with dual advantages of speed and manoeuverability, we propose an optimal interception scenario based on the LOS constraint. In this system, the LOS angles of the attack missile, the defence missile, and the aircraft are on the same straight line, as shown in Fig. 2. The defence missile is positioned between the attack missile and the aircraft such that it can intercept the attack missile and protect the aircraft.

In these circumstances, the relationship of relative motion among the three at the interception time can be described as:

$$\lambda_{AT}(t_f) = \lambda_{DT}(t_f) = \lambda_{AD}(t_f) \tag{15}$$

where t_f indicates the interception time.

Therefore, the guidance objective of the defence missile can be summarised as follows: By designing the guidance command a_D, the attack missile, defence missile and aircraft must satisfy $\lambda_{AT}(t_f) = \lambda_{DT}(t_f) = \lambda_{AD}(t_f)$ at the interception time to ensure the active defence of the aircraft.

Remark 1. As shown in Fig. 2, the guidance objective is formulated by simultaneously using information about the aircraft, attack missile and defence missile. It is designed to restrict the LOS of all three to ensure that the defence missile is always located in the mutual LOS during the flight, which also reflects the concept of cooperative guidance.

3.0 Design of active defence cooperative guidance law

To satisfy the guidance objective stated in Equation (15), the state variables $x_1 = \lambda_{AD} - \lambda_{AT}$ and $x_2 = \dot{\lambda}_{AD} - \dot{\lambda}_{AT}$ are selected to obtain the following guidance system:

$$\begin{cases} \boldsymbol{x} = [x_1 \ x_2]^T = \left[\lambda_{AD} - \lambda_{AT} \ \dot{\lambda}_{AD} - \dot{\lambda}_{AT}\right]^T \\ y = \lambda_{AD} - \lambda_{AT} \end{cases} \tag{16}$$

Based on Equations (11) and (12), we can obtain

$$\begin{aligned} \dot{x}_2 &= \ddot{\lambda}_{AD} - \ddot{\lambda}_{AT} \\ &= -\frac{2\dot{R}_{AD}\dot{\lambda}_{AD}}{R_{AD}} - \frac{a_D \cos(\gamma_D - \lambda_{AD})}{R_{AD}} + \frac{a_A \cos(\gamma_A - \lambda_{AD})}{R_{AD}} \\ &\quad + \frac{2\dot{R}_{AT}\dot{\lambda}_{AT}}{R_{AT}} - \frac{a_A \cos(\gamma_A - \lambda_{AT})}{R_{AT}} + \frac{a_T \cos(\gamma_T - \lambda_{AT})}{R_{AT}} \end{aligned} \tag{17}$$

This can be rewritten as

$$\begin{aligned} \dot{x}_2 &= \ddot{\lambda}_{AD} - \ddot{\lambda}_{AT} \\ &= f(\boldsymbol{x}, t) + b(t)a_D + d(t) \end{aligned} \tag{18}$$

where

$$f(\boldsymbol{x}, t) = -\frac{2\dot{R}_{AD}\dot{\lambda}_{AD}}{R_{AD}} + \frac{2\dot{R}_{AT}\dot{\lambda}_{AT}}{R_{AT}} \tag{19}$$

$$b(t) = -\frac{\cos(\gamma_D - \lambda_{AD})}{R_{AD}} \tag{20}$$

$$d(t) = \frac{a_A \cos(\gamma_A - \lambda_{AD})}{R_{AD}} - \frac{a_A \cos(\gamma_A - \lambda_{AT})}{R_{AT}} + \frac{a_T \cos(\gamma_T - \lambda_{AT})}{R_{AT}} \tag{21}$$

Assumption 1. *$d(t)$ represents the external disturbance or uncertainty of the system in Equation (18), and is related to the manoeuvering of the aircraft and the attack missile. It is assumed that $d(t)$ can be measured directly, and $|d(t)| \leq D_{\max}$, where $D_{\max}$ represents the upper bound of the external disturbance or uncertainty in the system.*

Based on Equations (15) and (16), we define the following nonlinear integral sliding surface to improve the property of the closed-loop error dynamic:

$$\sigma = x_2 + \int_0^t \left(K_P sig^{\alpha_1}(x_1) + K_V sig^{\alpha_2}(x_2) \right) dt \tag{22}$$

where $K_V = \omega_n^2$ and $K_P = 2\xi\omega_n(\omega_n > 0, 0 < \xi < 1)$ represent adjustable control gains related to the sliding surface, and $\Delta(x) = x^2 + K_V x + K_P$ is a Hurwitz polynomial. The nonlinear power function is $sig^{\alpha}(\cdot) = |\cdot|^{\alpha} \text{sgn}(\cdot)$, and $0 < \alpha_1 < 1, \alpha_2 = 2\alpha_1/(1 + \alpha_1)$.

Then, taking the derivative of Equation (22) with respect to time yields

$$\dot{\sigma} = \dot{x}_2 + K_p sig^{\alpha_1}(x_1) + K_V sig^{\alpha_2}(x_2) \tag{23}$$

The dynamic quality of the reaching motion of the sliding surface can be guaranteed by using reaching law [27, 28]. In a typical reaching law, there is a single reaching speed. Although the reaching speed of the exponential reaching law is high, chattering in the system is significant when it approaches the sliding surface. Although the power reaching law decreases this chattering to a certain extent, its rate of convergence is too low when the system is far from the sliding surface, and this results in a long reaching process. To overcome the deficiencies of the typical reaching law, we propose an improved reaching law as:

$$\dot{\sigma} = -\varepsilon|\sigma|^p \text{sign}(\sigma) - kf(\sigma) \tag{24}$$

where $p \in (0, 1)$, $\varepsilon, k \in \mathbb{R}^+$, and $f(\sigma)$ is a nonlinear function defined as

$$f(\sigma) = \begin{cases} \sigma & |\sigma| \le q \\ \text{sign}(\sigma) & |\sigma| > q \end{cases} \tag{25}$$

where $q \in \mathbb{R}^+$.

Combining Equation (23) with Equation (24), and substituting them into Equations (17) and (18) yields

$$\begin{aligned} \dot{\sigma} &= -\varepsilon|\sigma|^p \text{sign}(\sigma) - kf(\sigma) \\ &= \dot{x}_2 + K_p sig^{\alpha_1}(x_1) + K_V sig^{\alpha_2}(x_2) \\ &= f(\boldsymbol{x}, t) + b(t)a_D + d(t) + K_p sig^{\alpha_1}(x_1) + K_V sig^{\alpha_2}(x_2) \end{aligned} \tag{26}$$

Thus, the ADCG command a_D can be expressed as:

$$a_D = \frac{-\varepsilon|\sigma|^p \text{sign}(\sigma) - kf(\sigma) - f(\boldsymbol{x}, t) - d(t) - K_p sig^{\alpha_1}(x_1) - K_V sig^{\alpha_2}(x_2)}{b(t)} \tag{27}$$

Remark 2. As is shown in Equation (25), the improved reaching law consists of a power reaching term $-\varepsilon|\sigma|^p \text{sign}(\sigma)$ and a modified exponential reaching term $-kf(\sigma)$. A nonlinear function $f(\sigma)$ is introduced to the exponential reaching term; this can limit the amplitude when $|\sigma| > q$, and it is used to reduce the amplitude of the guidance command. When $|\sigma| \le q$, the state of the system approaches the sliding surface in an asymptotic process owing to the simple exponential approach, and this may not be attainable within a finite time. Therefore, a power reaching term is added to guarantee that the state of the system can reach the sliding surface in a finite time. In addition, because of the variable speed of the reaching performance of the power reaching term and the asymptotic characteristic of the exponential reaching term, the proposed reaching law can be used to reduce chattering in the guidance command.

Remark 3. The improved reaching law can ensure that the system has good reaching performance regardless of whether the state of the system is far from or close to the sliding surface. This can reduce chattering, and it is accessible within a finite time. This means that the state of the system can reach the sliding surface from any initial position within a finite time.

4.0 Stability analysis

Lemma 1. [29] *If, in the differential equation $f(x) = y' + p(x)y + q(x)y^n$ ($n \in \mathbb{R}^+$ is an arbitrary real number), $f(x) = aq(x)e^{-n \int p(x)dx}$ ($a \in \mathbb{R}$ is an arbitrary real number), the general solution of the differential equation is $y = u(x)e^{-\int p(x)dx}$, where $u(x)$ is determined by the separable variable equation $u'(x) = (a - u^n(x))q(x)e^{(1-n)\int p(x)dx}$.*

Lemma 2. [30] *For the following n-order system,*

$$
\begin{cases}
\dot{y}_1 = y_2 \\
\vdots \\
\dot{y}_{n-1} = y_n \\
\dot{y}_n = u
\end{cases}
\tag{28}
$$

if $\Delta(x) = x^n + K_n x^{n-1} + \cdots + K_2 x + K_1$ is a Hurwitz polynomial with $K_1, K_2, \cdots, K_n > 0$, then the n-order system can be stabilised in a finite time under the action of the control input u in Equation (29).

$$
u = -K_1 \mathrm{sig}^{\psi_1}(y_1) - K_2 \mathrm{sig}^{\psi_2}(y_2) - \cdots - K_n \mathrm{sig}^{\psi_n}(y_n)
\tag{29}
$$

where

$$
\psi_{i-1} = \frac{\psi_i \psi_{i+1}}{2\psi_{i+1} - \psi_i}(i = 2, 3, \cdots, n), \psi_n = \psi, \psi_{n+1} = 1
$$
$$
\varsigma \in (0, 1), \psi \in (1 - \varsigma, 1)
\tag{30}
$$

Theorem 1. *The nonlinear sliding surface σ can reach equilibrium, $\sigma = 0$, within a finite time $t_{\sigma 0 \to 0}$ from any initial position σ_0 under the action of reaching law in Equation (24), and*

$$
t_{\sigma_0 \to 0} = \frac{1}{k(p-1)} \ln \left(\frac{\dfrac{\varepsilon}{k}}{q^{1-p} + \dfrac{\varepsilon}{k}} \right) + \frac{(1+k)}{\varepsilon(1-p)} \left(\sigma_0^{1-p} - q^{1-p} \right)
\tag{31}
$$

Proof: The proof process can be divided into two steps. First, we prove the existence and accessibility of the improved reaching law in Equation (25). Second, we prove that the nonlinear sliding surface σ can reach equilibrium $\sigma = 0$ from any initial position σ_0 under the action of the improved reaching law in a finite time.

Step 1. Based on Equation (24), we can obtain

$$
\begin{aligned}
\sigma \dot{\sigma} &= \sigma(-\varepsilon|\sigma|^p \mathrm{sign}(\sigma) - kf(\sigma)) \\
&= -\varepsilon|\sigma|^{p+1} - kf(\sigma)\sigma
\end{aligned}
\tag{32}
$$

According to Equation (25), since $f(\sigma)$ is a piecewise nonlinear function, we classify and discuss the positive and negative forms of Equation (32).

Case 1. When $|\sigma| \leq q$, we can obtain

$$
\sigma \dot{\sigma} = -\varepsilon|\sigma|^{p+1} - k\sigma^2 \leq 0
\tag{33}
$$

The equality holds if and only if $\sigma = 0$.

Case 2. When $|\sigma| > q$,

$$
\sigma \dot{\sigma} = -\varepsilon|\sigma|^{p+1} - k|\sigma| \leq 0
\tag{34}
$$

The equality holds if and only if $\sigma = 0$.

Thus, $\sigma\dot{\sigma} \leq 0$ is established (the equality holds if and only if $\sigma = 0$). Based on the existence and accessibility conditions of the sliding-mode reaching law for continuous systems [31], it is easy to demonstrate that the proposed reaching law can ensure that the nonlinear sliding surface reaches equilibrium.

Step 2. We now classify and discuss the convergence time of the sliding surface based on Equation (25).

Case 1. When $0 \leq \sigma \leq q$ and $0 < p < 1$, the reaching law can be expressed as

$$\dot{\sigma} + k\sigma + \varepsilon\sigma^p = 0 \tag{35}$$

Based on Lemma 1, the general solution of Equation (35) can be presented as

$$\sigma = u\exp\left(-\int k\,\mathrm{d}t\right) \tag{36}$$

where u is determined by the variable separation in Equation (37).

$$u' = (0 - u^p)\,\varepsilon\exp\left((1-p)\int k\,\mathrm{d}t\right) \tag{37}$$

Solving Equation (37) yields

$$u = \left(c - \frac{\varepsilon}{k}\exp((1-p)kt)\right)^{\frac{1}{1-p}} \tag{38}$$

By substituting Equation (38) into Equation (36), we can obtain

$$\sigma^{1-p} = c\exp((p-1)kt) - \frac{\varepsilon}{k} \tag{39}$$

When $t = 0$ and $\sigma = q$, the constant c can be obtained as

$$c = q^{1-p} + (\varepsilon/k) \tag{40}$$

Therefore, based on Equation (39), the time needed by the nonlinear sliding surface to converge from $\sigma = q$ to $\sigma = 0$ can be described as

$$t_{q\to 0} = \frac{1}{k(p-1)}\ln\left(\frac{\dfrac{\varepsilon}{k}}{q^{1-p} + \dfrac{\varepsilon}{k}}\right) \tag{41}$$

Case 2. When $q \leq \sigma \leq \sigma_0$ and $0 < p < 1$, the reaching law can be expressed as

$$\dot{\sigma} = -\varepsilon\sigma^p - k \tag{42}$$

The homogeneous equation corresponding to Equation (42) can be expressed as

$$\dot{\sigma} + \varepsilon\sigma^p = 0 \tag{43}$$

Thus, σ can be expressed as

$$\sigma = [(-\varepsilon t + c)(1-p)]^{\frac{1}{1-p}} \tag{44}$$

Let c be a function of time t. We take the derivative of the above formula with respect to time to obtain

$$c(t) = -k\left(\frac{\sigma^{1-p}}{1-p} + c'\right) \tag{45}$$

where $c' \in \mathbb{R}$ is a constant number.

Combining Equations (44) with (45), we obtain

$$\sigma = \left[\left(-\varepsilon t - k\left(\frac{\sigma^{1-p}}{1-p} + c'\right)\right)(1-p)\right]^{\frac{1}{1-p}} \tag{46}$$

That is,

$$\frac{(1+k)\sigma^{1-p}}{1-p} = -\varepsilon t + c'' \tag{47}$$

where $c'' = -kc' \in \mathbb{R}$ is a constant number.

If $\sigma = \sigma_0$ when $t = 0$, we can obtain

$$c'' = \frac{(1+k)\sigma_0^{1-p}}{1-p} \tag{48}$$

According to Equation (47), when $0 < p < 1$, the time needed for convergence from $\sigma = \sigma_0$ to $\sigma = q$ is

$$t_{\sigma_0 \to q} = \frac{(1+k)}{\varepsilon(1-p)}\left(\sigma_0^{1-p} - q^{1-p}\right) \tag{49}$$

Thus, in combination with Equations (41) and (49), the time needed for the sliding surface to move from any initial state $\sigma = \sigma_0$ to equilibrium $\sigma = 0$ is

$$
\begin{aligned}
t_{\sigma_0 \to 0} &= t_{\sigma_0 \to q} + t_{q \to 0} \\
&= \frac{1}{k(p-1)}\ln\left(\frac{\dfrac{\varepsilon}{k}}{q^{1-p} + \dfrac{\varepsilon}{k}}\right) + \frac{(1+k)}{\varepsilon(1-p)}\left(\sigma_0^{1-p} - q^{1-p}\right)
\end{aligned}
\tag{50}
$$

Therefore, the sliding surface in Equation (22) can reach equilibrium $\sigma = 0$ from any initial state $\sigma = \sigma_0$ in a finite time under the proposed reaching law in Equation (24). Theorem 1 has thus been proved.

Theorem 2. *When the sliding surface in Equation (22) reaches equilibrium, $\sigma = 0$, x_1 and x_2 converge to zero in a finite time to ensure that the scenario involving the attack missile, defence missile and aircraft satisfies $\lambda_{AT}(t_f) = \lambda_{DT}(t_f) = \lambda_{AD}(t_f)$ at the interception time. This in turn implies that the active defence of the aircraft can be ensured.*

Proof. Once the sliding surface in Equation (22) reaches equilibrium, $\sigma = 0$, we can obtain

$$\sigma = x_2 + \int_0^t \left(K_p sig^{\alpha_1}(x_1) + K_V sig^{\alpha_2}(x_2)\right) dt = 0 \tag{51}$$

Taking the derivative of Equation (51) with respect to time yields

$$\dot{\sigma} = \dot{x}_2 + K_p sig^{\alpha_1}(x_1) + K_V sig^{\alpha_2}(x_2) = 0 \tag{52}$$

Then,

$$\dot{x}_2 = -K_p sig^{\alpha_1}(x_1) - K_V sig^{\alpha_2}(x_2) \tag{53}$$

Because $\dot{x}_1 = x_2$, and K_p, K_V, α_1, and α_2 are positive real numbers, we can use Lemma 2 to demonstrate that x_1 and x_2 can converge to zero in a finite time once the sliding surface in Equation (22) reaches equilibrium, $\sigma = 0$, and $\lambda_{AT}(t_f) = \lambda_{DT}(t_f) = \lambda_{AD}(t_f)$ can be established. Theorem 2 has thus been proved.

Table 1. *Initial conditions*

	Location (km)	V_i(m/s)	$\gamma_i(°)$	a_i^{max}(m/s^2)
A	(25,20)	1,800	225	150
D	(0,15)	900	15	100
T	(0,15)	400	5	25

Table 2. *Guidance parameters*

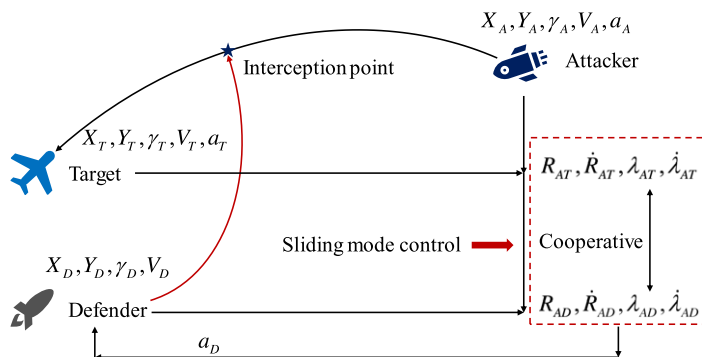| α_1	α_2	K_p	K_V	ε	k	p	q	N
0.6	0.75	5.6	16	0.2	0.1	0.5	0.0003	4

Figure 3. *Block diagram of the simulation.*

5.0 Simulation-based analysis

A block diagram of a simulation of the proposed ADCG law is shown in Fig. 3. To analyse the feasibility of the proposed guidance law, the initial conditions for the simulation of the attack missile, defence missile, and aircraft are set as shown in Table 1.

In all simulations, we assume that the attack missile attacks the aircraft under the action of the proportional navigation guidance (PNG) law in Equation (54). To verify the applicability of the ADCG law, four cases were simulated: different aircraft manoeuvering modes, different attack/defence missile speed ratios, different reaching laws applied to the ADCG law, and a robustness analysis of the ADCG law. The parameters of the guidance law in Equations (27) and (54) are shown in Table 2. To quantitatively analyse the advantages of the ADCG law, the energy consumed by the defence missile during interception is defined as $J = \int_0^t a_D{}^2 dt$.

$$(54)$$

$$a_A = N|\dot{R}_{AT}| \dot{\lambda}_{AT}$$

5.1 Different aircraft manoeuvering modes

In this subsection, we report the simulation of an aircraft moving with uniform speed and one performing a bang-bang manoeuver. In the two scenarios, the PNG and ADCG laws are used for comparative analysis. The results are shown in Tables 3–4 and Figs 4–5.

When the aircraft moves at a uniform speed along the initial heading direction, the PNG law is the optimal mode of attack for the attack missile [32]. Table 3 shows that both the ADCG and the PNG laws can be used to intercept the attack missile to protect the aircraft, but the former yields better interception of the attack missile. Compared with the PNG law, the interception time of the attack missile when using the ADCG law is 0.174s shorter, the interception accuracy is 48.64% higher, and the distance

Table 3. *Analysis of aircraft at uniform speed*

	Impact time (s)	R_{AD} (m)	R_{AT} (km)	J (m²/s³)
ADCG	9.654	0.8777	6.9439	3.1945×10^4
PNG	9.828	1.7090	6.7327	7.9567×10^4

Table 4. *Analysis of the aircraft adopting the bang-bang manoeuvering mode*

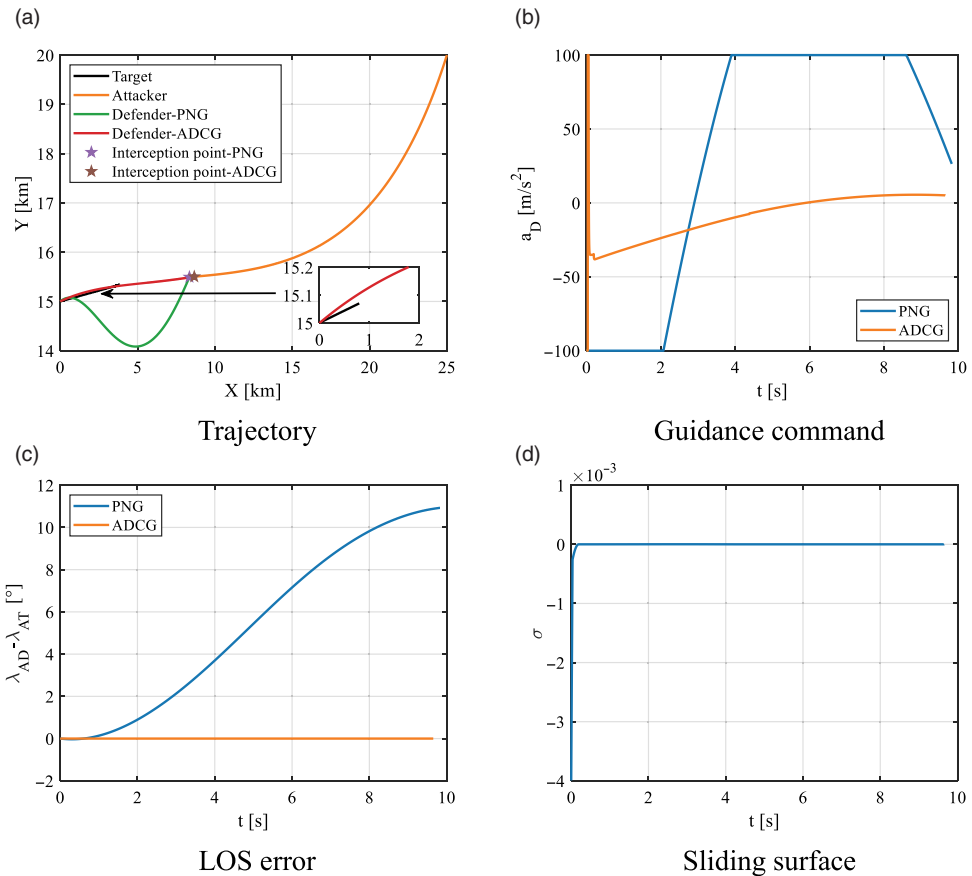|	Impact time (s)	R_{AD} (m)	R_{AT} (km)	J (m²/s³)
ADCG	9.934	0.8496	4.9086	3.9502×10^4
PNG	9.661	2.1868	4.3213	8.7711×10^4

Figure 4. *Results for the aircraft moving at a uniform speed.*

between the aircraft and the attack missile increases by 382.7m. Moreover, the defence missile consumes 4.7622×10^4 less energy when the ADCG law is used.

As shown in Fig. 4(a), when the ADCG law is used, the defence missile always moves along the LOS of the attack missile, defence missile and aircraft, and its trajectory appears to be smooth with a small curvature. Figure 4(b) shows that when the ADCG law is used, the guidance command of the defence missile briefly saturates in the initial stage of interception, and then it gradually and smoothly
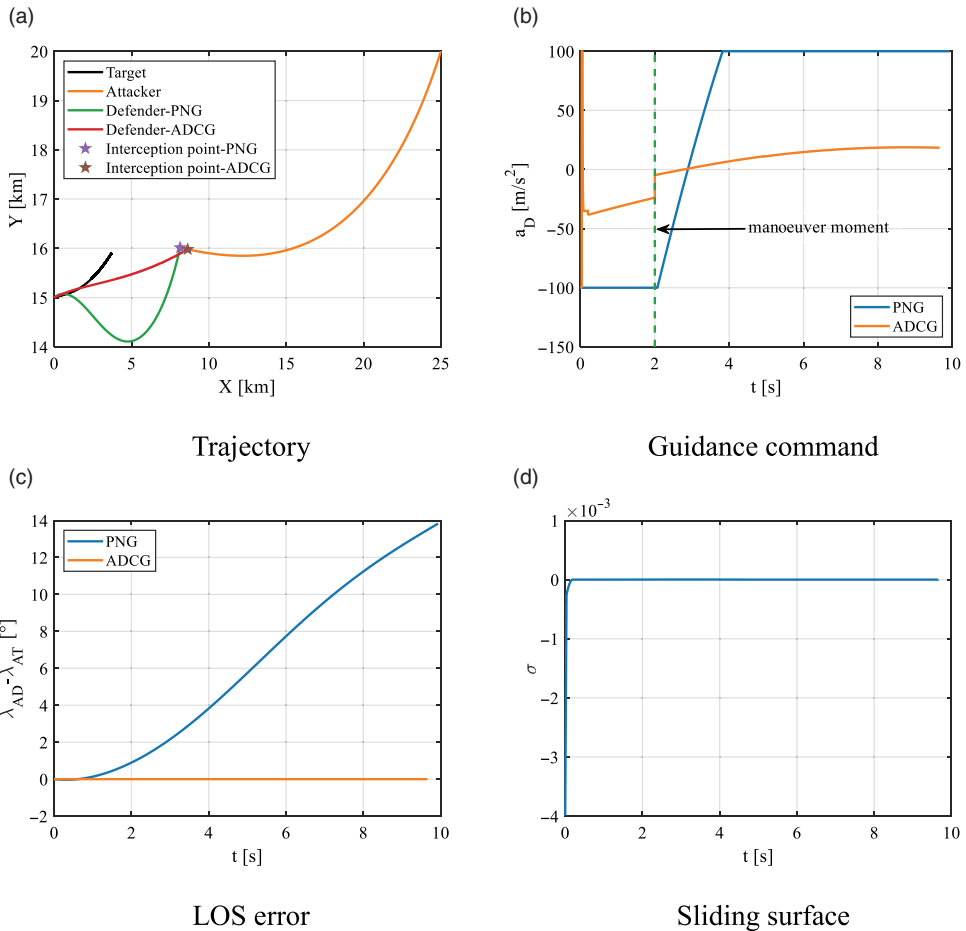
(a) Trajectory

(b) Guidance command

(c) LOS error

(d) Sliding surface

Figure 5. *Results of the aircraft adopting the bang-bang manoeuvering mode.*

decreases until the interception time of the attack missile. When the PNG law is used, the guidance command of the defence missile is saturated most of the time, and this significantly burdens to its actuator. Figure 4(c) shows that because information on the relative motion of the attack missile and the aircraft is simultaneously used by the defence missile, the value of $\lambda_{AT} - \lambda_{AD}$ is always close to zero, and the ideal interception by the defence missile can be ensured throughout the process of terminal guidance. Because the PNG law uses only unidirectional information between the attack and the defence missiles, $\lambda_{AT} - \lambda_{AD}$ increases with the guidance time, and it cannot realise ideal interception. According to Fig. 4(d), the sliding surface quickly converges to become close to zero, and there is no obvious chattering.

The bang-bang manoeuver is the optimal manoeuver for the aircraft to avoid danger [33]. Assuming that the aircraft has only one manoeuvering command switch, it uses the bang-bang manoeuvering mode at an acceleration of 20m/s^2 when the attack missile flies for 2s. As is shown in Table 4, when the aircraft uses the bang-bang manoeuver, the advantage of the ADCG law in terms of the interception of the attack missile is more prominent. Compared with the PNG law, the ADCG law used by the defence missile shortens the interception time by 0.273s, improves its accuracy by 61.15%, and increases the distance of between the aircraft and the attack missile by 587.3m. The defence missile also consumes 4.8209×104 less energy in this case.

Figure 5(a) shows that the defence missile is always on the LOS of the attack missile and the aircraft when the ADCG law is used. Figure 5(b) shows that when the defence missile uses the PNG law, the guidance command is saturated for the first two seconds, then exhibits a relationship of linear change with time, and finally reaches saturation, which imposes a significant burden on the actuator of the

Table 5. *Analysis of different values of μ*

μ	Impact time (s)	R_{AD} (m)	R_{AT} (km)	J (m^2/s^3)
1.5	8.688	0.8631	7.0094	6.5746×10^4
2	9.661	0.8496	4.9086	3.9502×10^4
2.5	10.364	0.4171	3.3982	3.3460×10^4
3	10.897	0.5690	2.2555	3.3681×10^4

defence missile. When the ADCG law is implemented, the guidance command of the defence missile is briefly saturated at the beginning, but then the saturation smoothly decreases. When $t=2$s, a jump in the guidance command occurs as the aircraft's manoeuvering mode is changed, and it then changes smoothly. Figure 5(c) shows that even if the aircraft uses the bang-bang manoeuver when applying the ADCG law, the value of $\lambda_{AT} - \lambda_{AD}$ remains close to zero, and the entire process of terminal guidance can ensure an optimal interception scenario. Figure 5(d) shows that the sliding surface quickly and smoothly converges to become close to zero.

5.2 Different attack/defence missile speed ratios

The simulation-based analysis in the previous section shows that, compared with the PNG law, the ADCG law has significant advantages in protecting the aircraft from an attack missile. In this section, we examine the performance of the ADCG law in terms of intercepting the attack missile at different ratios of its speed with respect to that of the defence missile, $\mu = V_A / V_D$. We assume that the aircraft uses the bang-bang manoeuvering mode. The results of this simulation are shown in Table 5 and Fig. 6.

As shown in Table 5, the defence missile can intercept the attack missile at different speed ratios to protect the aircraft using the ADCG scheme. Figure 6(a) shows that the defence missile always flies along the LOS of the attack missile, defence missile, and aircraft with a small ballistic curvature and a smooth trajectory. Figure 6(b) shows that, under the action of the ADCG law, the guidance command of the defence missile changes smoothly without obvious chattering. Figure 6(c) shows that because information on the relative motions of the attack missile and the aircraft is simultaneously used by the defence missile, the value of $\lambda_{AT} - \lambda_{AD}$ is always close to zero, and it is guaranteed to meet the constraint of ideal interception during the entire stage of terminal guidance. Figure 6(d) shows that the sliding surface quickly converges to become close to zero under different speed ratios without obvious chattering.

5.3 Using different reaching laws in the ADCG law

To verify the superiority of the improved reaching law when applied to the ADCG law, we conducted comparative simulations using a constant reaching law (CRL) and an exponential reaching law (ERL) to design the guidance laws. The corresponding guidance laws were designed as follows.

- ADCG law based on CRL:

$$a_D = \frac{-\varepsilon_1 \text{sign}(\sigma) - f(\boldsymbol{x}, t) - d(t) - K_p sig^{\alpha_1}(x_1) - K_V sig^{\alpha_2}(x_2)}{b(t)} \tag{55}$$

- ADCG law based on ERL:

$$a_D = \frac{-\varepsilon_2 \text{sign}(\sigma) - k_1 \sigma - f(\boldsymbol{x}, t) - d(t) - K_p sig^{\alpha_1}(x_1) - K_V sig^{\alpha_2}(x_2)}{b(t)} \tag{56}$$

Table 6. *Analysis of different reaching laws*

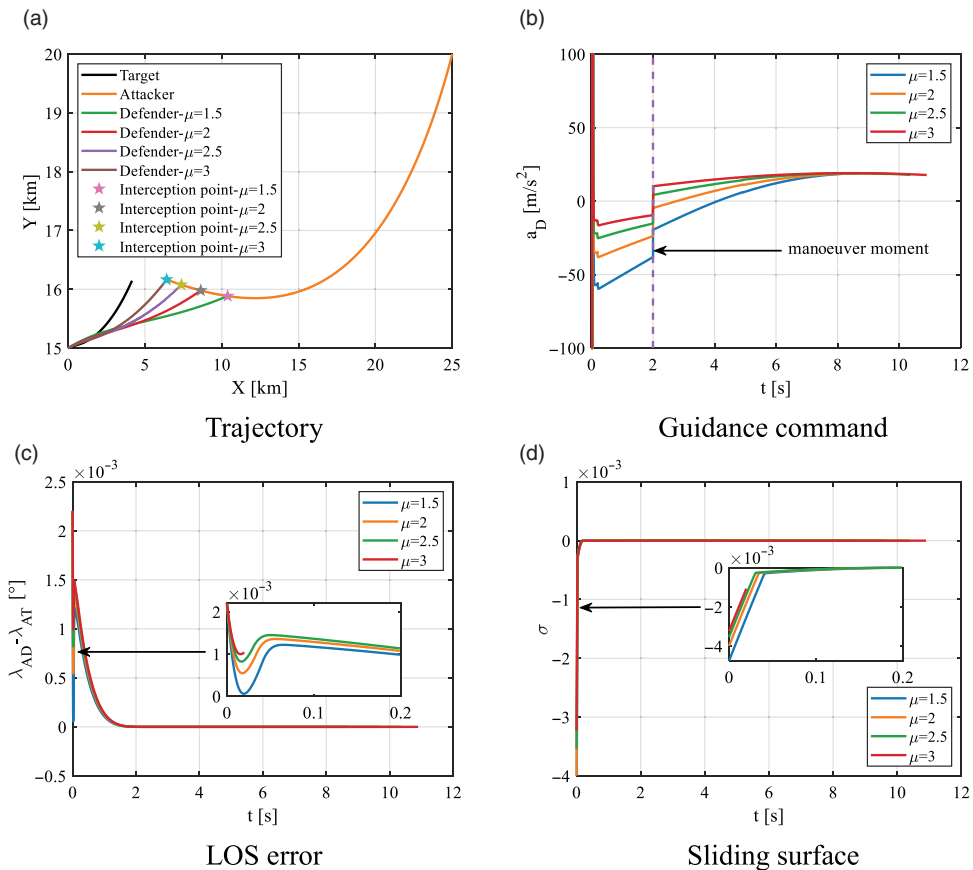|	R_{AD} (m)	R_{AT} (km)	J (m²/s³)
CRL	0.8632	4.9086	9.5457×10^4
ERL	0.8753	4.9086	4.9290×10^4
Proposed	0.8496	4.9088	3.9502×10^4

Figure 6. *Results of different values of μ.*

The guidance parameters in Equations (55) and (56) were set to $\varepsilon_1 = \varepsilon_2 = 0.01$ and $k_1 = 0.1$, and we assumed that the defence missile used the bang-bang manoeuvering mode. The results are shown in Table 6 and Fig. 7. Table 6 shows that the defence missile intercepts the attack missile under the action of different reaching laws to protect the aircraft. However, the improved reaching law has higher interception accuracy than the CRL and ERL. Figure 7(a) shows that the use of different reaching laws yields no significant differences in the trajectory of the defence missile. Figure 7(b) shows that the improved reaching law weakens chattering in the guidance command to reduce the burden on the actuator of the defence missile. Figure 7(c) shows that $\lambda_{AT} - \lambda_{AD}$ is always close to zero, so the defence missile is guaranteed to satisfy the conditions of ideal interception during the entire stage of terminal guidance. However, the improved reaching law increases the speed of convergence, and the change is smoother. Figure 7(d) shows that, compared with the CRL and ERL, the improved reaching law converges to become close to zero more quickly, and there is no obvious chattering.
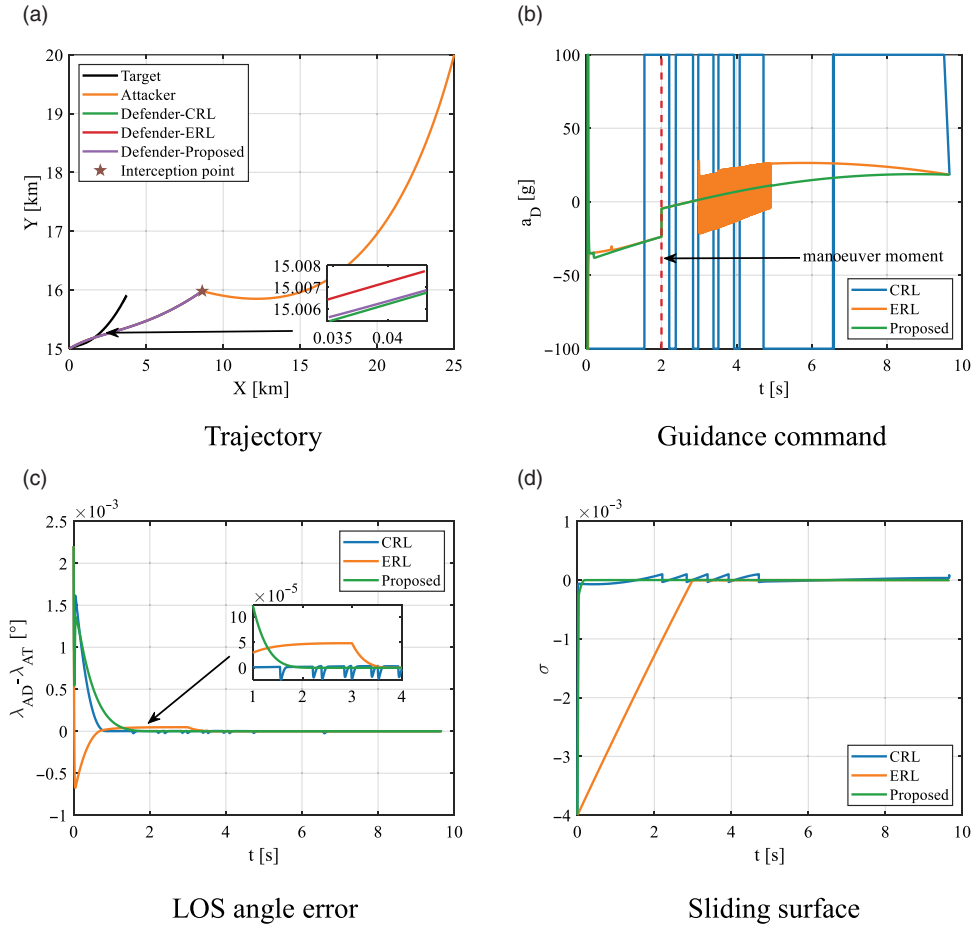
(a)

Trajectory

(b)

Guidance command

(c)

LOS angle error

(d)

Sliding surface

Figure 7. *Results of different reaching laws.*

5.4 Monte Carlo simulations

To further verify the robustness of the proposed guidance system, we ran 200 Monte Carlo simulations of the trajectory set by the proposed guidance system in the presence of measurement errors, and we statistically analysed the results. The aircraft was again assumed to have used the bang-bang manoeu-vering mode. The simulations were conducted supposing that errors in the measurement of the relative speeds of $\dot{R}_{AT}$ and $\dot{R}_{AD}$ obey a Gaussian distribution, with a mean of zero and a variance of 1m/s, and that $\dot{\lambda}_{AT}$ and $\dot{\lambda}_{AD}$ obey a Gaussian distribution with a mean of zero and a variance of 0.01rad/s. The results are shown in Fig. 8.

The data of the Monte Carlo experiment show that the average miss distances of the attack missile relative to the defence missile and the aircraft are 1.3001m and 4.7442 km, respectively, and the standard deviations are 0.2559 m and 0.2995 km. This meets the interception accuracy requirements to ensure the safe flight of the aircraft. Moreover, the average error of $\lambda_{AD} - \lambda_{AT}$ is -0.0116°, with a standard deviation of 0.0137°. This can ensure optimal interception. Thus, the proposed ADCG law is highly robust in the presence of errors and noise.

6.0 Conclusion

To address the problems of using a cheap and low-speed airborne defence missile with low manoeuver-ability to accurately intercept a fast and expensive attack missile with high manoeuverability to protect
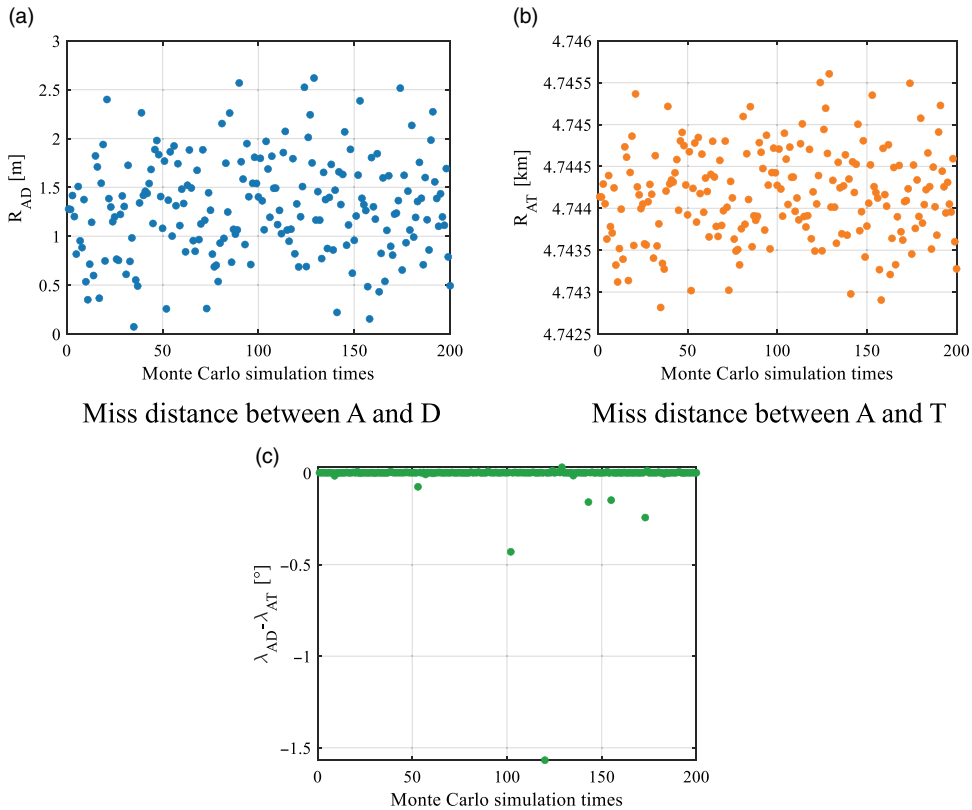
(a)

Miss distance between A and D

(b)

Miss distance between A and T

(c)

Error in the LOS angle between λ_{AD} and λ_{AT}

Figure 8. *Results of Monte Carlo simulations.*

the safety of an aircraft, an ADCG law is proposed based on SMC method and the concept of the LOS constraint. The main conclusions can be summarised as follows.

(1) The proposed guidance law can ensure that the defence missile always moves in the line of LOS between of the aircraft and the attack missile so that the safety of the aircraft can be guaranteed.

(2) A defence missile guided by the ADCG law can effectively intercept the attack missile under different attack/defence missile speed ratios, showing great value in engineering practice.

(3) Compared with other guidance laws, the ADCG law shows great advantages in terms of convergence speed and robustness in the presence of errors and noise.

Conflicts of interest. The authors declare that they have no known competing financial interests or personal relationships that could have appeared to influence the work reported in this paper

Supplementary material. To view supplementary material for this article, please visit https://doi.org/10.1017/aer.2022.62.

References

[1] Yan, X. and Lyu, S. A two-side cooperative interception guidance law for active air defense with a relative time-to-go deviation, *Aerospace Sci. Technol.*, 2020, **100**, 105787.

[2] Zhao, Z.T., Huang, W., Yan, L. and Yang, Y.G. An overview of research on wide-speed range waverider configuration, *Progr. Aerospace Sci.*, 2020, **113**, 100606.

[3] Zhang, T., Yan, X., Huang, W., Che, X. and Wang, Z. Multidisciplinary design optimization of a wide speed range vehicle with waveride airframe and RBCC engine, *Energy*, 2021, **235**, 121386.

[4] Weiss, M., Shima, T., Castaneda, D. and Rusnak, I. Combined and cooperative minimum-effort guidance algorithms in an active aircraft defense scenario, *J. Guidance Control Dyn.*, 2017, **40**, (5), pp 1241–1254.

[5] Garcia, E., Casbeer, D.W., Fuchs, Z.E. and Pachter, M. Cooperative missile guidance for active defense of air vehicles, *IEEE Trans. Aerospace Electron. Syst.*, 2017, **54**, (2), pp 706–721.

[6] Han, T., Hu, Q. and Xin, M. Three-dimensional approach angle guidance under varying velocity and field-of-view limit without using line-of-sight rate, *IEEE Trans. Syst. Man Cybern. Syst.*, 2022, Published Online, doi: 10.1109/TSMC.2022.3150299

[7] Han, T., Shin, H.-S., Hu, Q., Tsourdos, A. and Xin, M. Differentiator-based incremental three-dimensional terminal angle guidance with enhanced robustness, *IEEE Trans. Aerospace Electron. Syst.*, 2022, Published Online, doi: 10.1109/TAES.2022.3158639

[8] Shima, T. Optimal cooperative pursuit and evasion strategies against a homing missile, *J. Guidance Control Dyn.*, 2011, **34**, (2), pp 414–425.

[9] Shaferman, V. and Shima, T. Cooperative multiple-model adaptive guidance for an aircraft defending missile, *J. Guidance Control Dyn.*, 2010, **33**, (6), pp 1801–1813.

[10] Prokopov, O. and Shima, T. Linear quadratic optimal cooperative strategies for active aircraft protection, *J. Guidance Control Dyn.*, 2013, **36**, (3), pp 753–764.

[11] Perelman, A., Shima, T. and Rusnak, I. Cooperative differential games strategies for active aircraft protection from a homing missile, *J. Guidance Control Dyn.*, 2011, **34**, (3), pp 761–773.

[12] Saurav, A., Kumar, S.R. and Maity, A. Cooperative guidance strategies for aircraft defense with impact angle constraints, AIAA Scitech 2019 Forum, 2019, p 0356.

[13] Rubinsky, S. and Gutman, S. Three-player pursuit and evasion conflict, *J. Guidance Control Dyn.*, 2014, **37**, (1), pp 98–110.

[14] Naiming, Q.I., Qilong, S.U.N. and Jun, Z.H.A.O. Evasion and pursuit guidance law against defended target, *Chin. J. Aeronaut.*, 2017, **30**, (6), pp 1958–1973.

[15] Qilong, S.U.N., Naiming, Q.I., Longxu, X.I.A.O. and Haiqi, L.I.N. Differential game strategy in three-player evasion and pursuit scenarios, *J. Syst. Eng. Electron.*, 2018, **29**, (2), pp 352–366.

[16] Ratnoo, A. and Shima, T. Line-of-sight interceptor guidance for defending an aircraft, *J. Guidance Control Dyn.*, 2011, **34**, (2), pp 522–532.

[17] Yamasaki, T., Balakrishnan, S.N. and Takano, H. Geometrical approach-based defense-missile intercept guidance for aircraft protection against missile attack, *Proc. Inst. of Mech. Eng. Part G J. Aerospace Eng.*, 2012, **226**, (8), pp 1014–1028.

[18] Ratnoo, A. and Shima, T. Line of sight guidance for defending an aircraft, AIAA Guidance, Navigation, and Control Conference, 2010, p 7877.

[19] Liu, S., Liu, W., Yan, B., Liu, S. and Yin, Y. Impact time control guidance law for large initial lead angles based on sliding mode control, *J. Phys. Conf. Ser.*, 2021, **2031**, (1), 012050.

[20] Han, T., Hu, Q., Shin, H.S., Tsourdos, A. and Xin, M. Sensor-based robust incremental three-dimensional guidance law with terminal angle constraint, *J. Guidance Control Dyn.*, 2021, **44**, (11), pp 2016–2030.

[21] Liu, S., Yan, B., Liu, R., Dai, P., Yan, J. and Xin, G. Cooperative guidance law for intercepting a hypersonic target with impact angle constraint, *Aeronaut. J.*, 2022, **126**, (1300), 1026–1044.

[22] Liu, S., Yan, B., Zhang, T., Dai, P. and Yan, J. Guidance law with desired impact time and FOV constrained for antiship missiles based on equivalent sliding mode control, *Int. J. Aerospace Eng.*, 2021. doi: 10.1155/2021/9923332

[23] Shin, H.S., Tsourdos, A. and Li, K.B. A new three-dimensional sliding mode guidance law variation with finite time convergence, *IEEE Trans. Aerospace Electron. Syst.*, 2017, **53**, (5), pp 2221–2232.

[24] Song, J. and Song, S. Three-dimensional guidance law based on adaptive integral sliding mode control, *Chin. J. Aeronaut.*, 2016, **29**, (1), pp 202–214.

[25] Sinha, A. and Kumar, S.R. Supertwisting control-based cooperative salvo guidance using leader–follower approach, *IEEE Trans. Aerospace Electron. Syst.*, 2020, **56**, (5), pp 3556–3565.

[26] Liu, S., Yan, B., Zhang, X., Liu, W. and Yan, J. Fractional-order sliding mode guidance law for intercepting hypersonic vehicles, *Aerospace*, 2022, **9**, (2), p 53.

[27] Shtessel, Y., Taleb, M. and Plestan, F. A novel adaptive-gain supertwisting sliding mode controller: Methodology and application, *Automatica*, 2012, **48**, (5), pp 759–769.

[28] Qian, D. and Yi, J. *Hierarchical Sliding Mode Control for Under-Actuated Cranes*, Springer, 2016, Heidelberg, Berlin.

[29] Lian Fu, L. Application and ordinary solution of a kind of first order differential equation, *J. Huangshi Inst. Technol.*, 2011, **27**, (4), pp 41–42 (in Chinese).

[30] Bhat, S.P. and Bernstein, D.S. Geometric homogeneity with applications to finite-time stability, *Math. Control Signals Syst.*, 2005, **17**, (2), pp 101–127.

[31] Chalanga, A., Kamal, S., Fridman, L.M., Bandyopadhyay, B. and Moreno, J.A. Implementation of super-twisting control: Super-twisting and higher order sliding-mode observer-based approaches, *IEEE Trans. Indus. Electron.*, 2016, **63**, (6), pp 3677–3685.

[32] Shima, T. and Golan, O.M. Linear quadratic differential games guidance law for dual controlled missiles, *IEEE Trans. Aerospace Electron. Syst.*, 2007, **43,** (3), pp 834–842.

[33] Shinar, J. and Steinberg, D. Analysis of optimal evasive maneuvers based on a linearized two-dimensional kinematic model, *J. Aircraft*, 1977, **14,** (8), pp 795–802.